島根大学地球資源環境学研究報告　23, 27～37 ページ（2004 年 12 月）
Geoscience Rept. Shimane Univ., 23, p.27～37（2004）

Article

Major and trace element abundances in the <180μm and sand fractions of stream sediments from the Hino River, Tottori, Japan

Edwin Ortiz* and Barry P. Roser*

Abstract

X-ray fluorescence analyses for major elements and 14 trace elements were made of both the <180μm and sand fractions of 103 stream sediment samples collected from active channels of the Hino River, west Tottori Prefecture. Combined histograms of elemental abundances show clear dependence of composition on grain size, with the fine factions containing greater abundances of all elements except SiO_2, K_2O, Ba, Pb, and Rb. Distributions are representative of fractions taken from river sediments, with mainly positively skewed patterns. Bimodal or polymodal distributions in the sand fractions for a number of elements (Sr, SiO_2, K_2O, Al_2O_3, CaO, Na_2O, and Rb) reflect the influence of local source rocks on composition, as one of the modes is related to samples with catchments draining Mount Daisen. Variation diagrams also clearly display fractionation between the fine and sand fractions. The results show that samples originating from Mount Daisen are the most distinctive, especially with respect to high Sr abundances and relatively low Y, which reflect the adakitic nature of the source volcanics. Intermediate abundances in samples from the lower main channel reflect mixing and homogenization of detritus from two areas with contrasting lithologies, felsic granitoids and volcanics to the south, and volcanic products from Daisen to the northeast. Values of Cr are high in the upper reaches of the main channel, reflecting a strong provenance fingerprint from ultrabasic rocks. Abundances of this element then decrease steadily downstream due to dilution from Cr-poor lithotypes.

Key words: Geochemistry, stream sediments, <180μm fraction, sand fraction, Daisen products, granitoids, Hino River, Tottori.

Introduction

The geochemical compositions of modern stream sediments mainly reflect the chemical characteristics of the source lithotypes and derived soils contained in their catchments, and the influence of weathering, transport, sorting, and post-depositional processes. Studies of stream sediments have potential application in varied geological and geoenviromental research. This article presents the results of X-ray fluorescence (XRF) analysis of both fine (<180μm) and sand fractions (180-2000μm) of 103 stream sediments collected from the Hino River in the northern San-in District.

The Hino River catchment drains an area of about 860 km^2, and is located in west Tottori Prefecture, where its watershed constitutes the boundary with Shimane Prefecture. Study of the Hino River catchment and characterization of the sediments within it is of direct relevance to other work examining development of Yumigahama Peninsula related to past tatara mining, and of dispersion paths of sediments in Miho Bay.

The object of this report is to present the raw data obtained by XRF analysis, and to outline some of the general relations between abundances of elements in fractions of the bulk sediments from the Hino River. More detailed interpretation of the results will be published later. The dataset reported in this paper constitutes another step toward achieving a regional geochemical database for the northern San-in area. This work began with study of the Kando River (Ortiz and Roser, 2003; Ortiz and Roser, *this volume*), and is intended to extend to the Hii River.

Geological Outline

Most of the catchment area of the Hino River is occupied by felsic geological units, mainly Cretaceous to Paleogene granitoids and coeval volcanic rocks (Fig. 1). The granitoids are distributed throughout the central and southern regions of the watershed, and comprise granites, granite porphyries, diorites, granodiorites and gabbros. In contrast, the coeval volcanic rocks crop out mainly on the edges of the watershed, especially towards the southwest (Japan Institute of Construction Engineering "JICE", 1984; EBGMSP, 1997). Lithotypes include rhyolite, quartz andesite, andesite, and pyroclastics. Outcrops of several other less extensive units are scattered across the area (Fig. 1). These include Sangun Group ultrbasic-basic, calcareous, siliceous, and psammitic schists; Miocene-Pliocene augite basalts, olivine andesite lavas and pyroclastics; and Miocene to Jurassic sedimentary rocks (JICE, 1984).

Most of the rocks and units outlined above have been examined in varying detail during regional mapping or more specific studies of aspects such as granitoid petrogenesis (e.g., Ota, 1962; Hattori and Katada, 1964; Hashimoto, 1973; 1990; Hattori and Shibata, 1974; Murakami, 1974; Iizumi *et al.,* 1984; 2000; Research Group

*Dept. of Geoscience, Shimane University, Matsue 690-8504, Japan

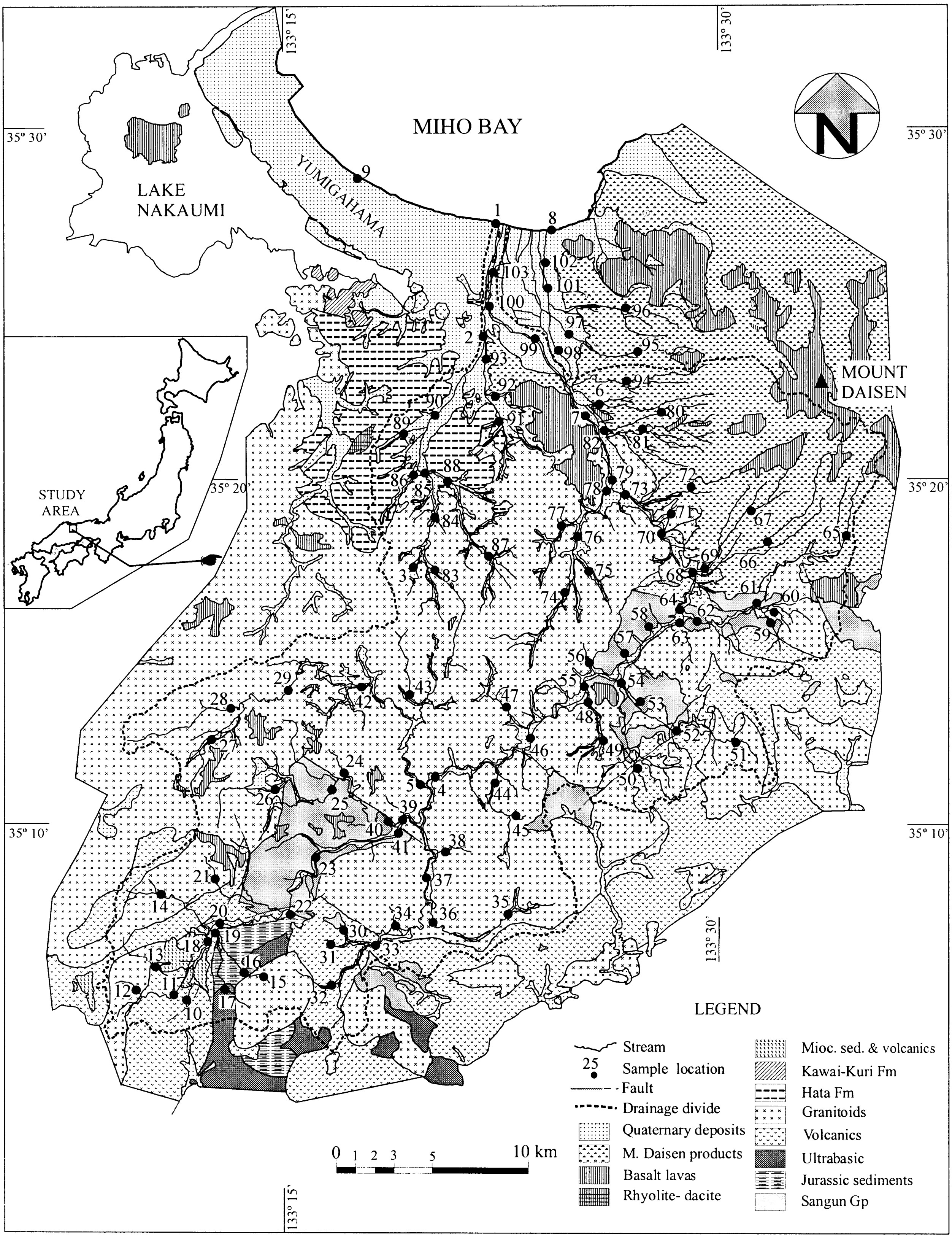

Fig. 1. Map showing the generalized distribution of lithotypes in the catchment of the Hino River and location of sample sites. Geology based on the 1:200,000 geological maps of Chugoku Area No 3 (Japan Institute of Construction Engineering, 1984) and Shimane Prefecture (Editorial Board of the Geological map of Shimane Prefecture, 1997).

for the Batholith in the San'in Zone, 1982; Nagao *et al.*, 1990).

The geology in the downstream reaches consists of different lithotypes. Rhyolites, andesites, and andesitic pyroclastic rocks of the Hata Formation (EBGMSP, 1997) crop out in the northwest. Conversely, volcanic products associated with Mount Daisen dominate the northeastern corner of the study area. Daisen products include andesite to quartz andesite pyroclastics, websterites, amphibolite andesites, tuff-breccias, lapilli and volcanic ash deposits, among others. Several studies have examined the distribution of Daisen rocks and their characteristics (e.g., Ota, 1959; Miura *et al.*, 1991; Morris, 1995; Kimura *et al.*, 1999, 2003).

Considerable contrasts in source rock compositions thus exist within the catchment of the Hino River. For example, about one third of the total length of the main channel (corresponding to the lower reaches) receives material almost exclusively derived from the western flank of Mount Daisen. The rest of the main channel is primarily fed from felsic source rocks. Any modification of the drainage (e.g., dams, artificial channels) at specific locations could thus lead to changes in the chemical composition of detritus reaching Miho Bay. Such modification has occurred in the past, with massive influx of granitoid waste from historic tatara mining leading to accelerated growth of Yumigahama Peninsula.

Sampling and Sample Preparation

Field sampling

Field work to collect the stream sediments was carried on nine days in October and early November, 2003. Weather conditions were generally fine, and streams clear. Composite samples were collected with a plastic water scoop from active channels, and stored in plastic zip-top bags. Where possible, samples were taken from both sides of the streams over a channel length of 10-30 m.

An array of sampling sites was selected with the aim of establishing a uniform distribution that would cover all source lithologies present. Sites were identified on 1:50,000 topographic maps, according to the lithotypes present from the 1:200,000 geological maps of western Tottori and Shimane Prefectures (JICE, 1984; EBGMSP, 1997).

Samples were collected from 103 sites in the Hino catchment (Fig. 1), numbered in order of collection. Some sampling sites had to be displaced from the location originally planned due to unfavorable conditions, including lack of access, disturbance by current construction projects, or simply because of paucity of sand-sized sediment. The overall sampling density was one sample per 8.3 km^2.

Sample preparation

Bulk samples were dried at 80-90℃ the day after collection. Dried bulk samples were than passed through an 8.6 mesh sieve to remove material coarser than 2 mm. Average weight of the <2 mm fractions was 1342 g. These were then split into manageable portions using a simple aluminium chute, and these later put through an 83 mesh stainless steel sieve to separate the <180 μm (fine fraction) and the 180-2000 μm (sand) fraction. For most samples, sieving of an eighth or quarter split was sufficient to provide enough <180 μm material for the XRF analysis. For six samples, half the bulk <2 mm fraction had to be used, and for one particularly well-sorted sample three quarters of the bulk material was sieved. On average, the fine fractions comprised 12.1 wt% of the <2 mm bulk fraction. Only in ten samples did the fine fraction exceed 30 wt%.

The fine and sand fractions were then separately crushed in tungsten carbide mills. The fine fractions were crushed in a small puck mill for about 10-15 seconds, in loads of 12-20 g, whereas the sand fractions were crushed in a larger ring mill for 30 seconds, in loads ranging between 50 and 150 g. Subsamples (7-10 g) of the crushed material were then stored in glass vials and dried at 110℃ for at least 24 hours before determination of loss on ignition (LOI).

Analytical Methods

Gravimetric LOI was determined for each sample from the net weight loss after ignition in a muffle furnace at 1000 ℃ for two hours. The ignited materials were then manually disaggregated in an agate pestle and mortar, and returned to a 110℃ oven for at least 24 hours prior to the preparation of fusion beads for X-ray fluorescence analysis (anhydrous basis).

Major elements and 14 trace elements (Ba, Ce, Cr, Ga, Nb, Ni, Pb, Rb, Sc, Sr, Th, V, Y, Zr) were determined using a Rigaku RIX-2000 XRF at Shimane University. All analyses were carried out on fused glass beads prepared with an alkali flux comprising 80% lithium tetraborate and 20% lithium metaborate. The flux to sample ratio was 2:1. The analytical methods, instrumental conditions, and calibrations used were those described by Kimura and Yamada (1996). Analyses were monitored using new beads for seven GSJ and USGS standards. More detailed descriptions of the methods utilized in this study are given by Roser *et al.* (2000, 2001) and Ortiz and Roser (2003).

Results and Discussion

Major and trace element results for the fine fractions and the sand fractions are given in Tables 1 and 2 respectively, reported on a hydrous basis. LOI values in the fine fractions were generally <10 wt%, but occasional higher values (>10%) suggest that some samples are enriched in organic matter. In contrast, LOI values for the sand fractions are considerably lower, with most <3 wt %. Only six samples have higher values, ranging up to 5.7 wt %.

Summary statistics for the fine and sand fractions are

Table 1. Major and trace element analyses of the <180 μm fraction, Hino River (hydrous basis). Major elements wt %, trace elements ppm.

SaNr	TYPE	SiO_2	TiO_2	Al_2O_3	Fe_2O_3T	MnO	MgO	CaO	Na_2O	K_2O	P_2O_5	LOI	SUM	Ba	Ce	Cr	Ga	Nb	Ni	Pb	Rb	Sc	Sr	Th	V	Y	Zr	% Fines
HN-1F	MCBDPI	58.29	0.78	14.48	5.16	0.17	1.80	2.59	4.36	2.79	0.16	8.55	99.12	324	72	150	11	10	33	8	93	10.3	325	14.8	118	36	317	1.0
HN-2F	HI	63.22	0.68	17.46	4.64	0.17	0.93	1.64	3.19	2.73	0.16	5.14	99.96	382	88	26	19	12	12	19	99	10.1	197	19.0	73	44	314	52.5
HN-3F	GDP	61.38	0.74	18.66	5.74	0.11	1.34	1.92	4.28	2.45	0.10	3.50	100.21	306	86	57	21	12	21	16	89	11.2	233	27.0	96	39	404	5.9
HN-4F	GDP	60.47	1.98	13.29	11.14	0.25	2.05	2.44	2.63	2.49	0.12	2.23	99.08	363	119	2052	17	19	53	18	87	15.1	185	26.7	307	53	755	16.9
HN-5F	GDP	70.87	0.35	14.27	2.32	0.08	0.61	1.30	3.89	3.84	0.04	1.56	99.14	320	92	161	17	11	13	408	148	5.6	116	26.4	33	23	205	12.6
HN-6F	DP	56.56	0.83	18.92	7.00	0.12	2.49	4.62	3.29	1.13	0.17	4.74	99.86	293	47	48	21	7	27	12	34	14.3	653	4.1	132	14	238	6.9
HN-7F	MCBDPI	59.63	0.87	16.62	7.07	0.16	2.58	4.39	3.29	1.78	0.15	2.93	99.46	312	59	266	19	9	39	18	61	14.2	504	10.8	143	24	241	7.6
HN-10F	A	59.84	0.59	15.71	4.28	0.11	1.43	1.84	1.53	2.76	0.12	11.53	99.75	507	71	372	12	9	42	9	111	8.8	233	10.4	65	23	271	9.1
HN-11F	GDP	63.14	0.58	15.33	4.07	0.08	0.91	1.37	1.88	3.40	0.08	8.67	99.51	457	67	72	16	10	12	10	139	9.5	214	11.8	54	26	287	11.2
HN-12F	GDP	63.65	0.64	15.97	4.38	0.10	0.93	1.49	1.89	3.46	0.07	7.31	99.90	444	87	138	20	12	18	24	144	7.6	219	16.2	74	30	500	5.0
HN-13F	GDP	62.27	0.67	14.33	4.45	0.14	0.82	1.67	2.12	3.04	0.10	10.37	99.97	502	65	52	16	10	16	11	117	7.9	186	11.3	78	27	314	4.3
HN-14F	GDP	66.99	0.50	15.30	3.94	0.13	1.00	2.06	3.18	2.67	0.10	3.67	99.53	508	74	190	16	9	15	21	106	8.9	194	11.3	55	29	305	23.1
HN-15F	GDP	66.59	0.45	15.20	4.17	0.09	0.88	1.44	1.73	4.12	0.08	4.94	99.68	401	74	125	17	7	15	22	176	11.7	165	14.5	57	25	459	13.2
HN-16F	GDP	55.88	1.00	16.67	7.50	0.17	2.17	2.87	2.43	2.52	0.17	8.29	99.67	362	79	997	20	11	132	16	106	21.1	221	14.4	120	46	547	11.2
HN-17F	GDP	48.47	0.98	14.83	8.56	0.16	8.38	2.69	1.60	1.67	0.16	9.72	97.20	306	9	7425	18	8	650	15	68	17.9	179	9.0	181	31	283	15.7
HN-18F	GDP	61.35	1.39	13.84	7.91	0.16	2.17	1.86	1.96	2.76	0.11	5.34	98.85	409	56	3193	17	12	121	24	103	11.0	205	10.5	197	25	460	5.1
HN-19F	GDP	56.81	0.81	15.79	6.73	0.14	3.57	2.89	2.48	2.36	0.16	7.16	98.89	348	47	4173	18	9	283	13	96	18.1	219	11.1	118	35	360	2.0
HN-20F	GDP	59.78	0.70	15.75	5.61	0.13	2.32	2.59	2.29	2.40	0.15	7.90	99.63	428	56	1992	18	8	126	16	92	14.3	210	9.5	99	30	250	4.4
HN-21F	GDP	57.60	1.46	15.37	10.52	0.24	2.64	3.96	2.89	1.75	0.17	3.27	99.86	379	74	261	17	11	16	18	61	23.8	236	8.6	282	36	526	9.7
HN-22F	GDP	51.57	0.81	14.37	7.31	0.13	4.76	2.26	1.56	1.67	0.16	14.76	99.35	361	42	1724	15	8	331	4	60	15.6	212	6.3	135	25	172	15.4
HN-23F	GDP	48.95	2.98	11.37	20.64	0.35	3.04	2.37	1.90	1.98	0.15	2.97	96.70	336	43	6213	18	18	141	19	64	13.9	170	10.4	652	29	542	3.1
HN-24F	GDP	66.13	0.61	17.69	2.01	0.17	0.68	1.61	3.82	4.62	0.05	1.99	99.38	351	217	29	19	21	11	11	174	7.7	188	82.1	36	120	333	13.1
HN-25F	GDP	55.79	1.85	12.92	16.43	0.36	1.88	2.65	2.87	1.80	0.13	2.74	99.41	388	104	270	17	17	19	13	56	18.9	192	16.0	363	43	1013	12.8
HN-26F	GDP	57.10	1.40	15.30	12.58	0.31	1.31	2.36	3.79	2.09	0.10	3.44	99.79	439	106	328	19	20	22	19	67	12.9	190	13.5	234	40	744	2.7
HN-27F	GDP	57.83	0.86	17.51	8.15	0.31	1.38	2.48	3.08	2.45	0.17	6.00	100.22	505	95	131	20	12	25	16	85	18.9	223	19.6	140	45	555	4.9
HN-28F	GDP	59.44	0.64	19.44	4.75	0.17	1.15	2.30	4.13	2.63	0.08	5.23	99.95	332	97	34	22	14	10	13	105	14.8	199	29.3	77	41	560	7.5
HN-29F	GDP	62.64	0.80	17.68	5.89	0.17	1.35	2.53	3.98	2.68	0.05	2.43	100.21	353	125	64	20	16	8	12	99	18.5	184	36.4	111	53	682	37.4
HN-30F	GDP	56.96	0.84	17.32	6.83	0.15	2.21	2.95	2.04	2.36	0.16	8.08	99.92	398	72	123	18	9	66	12	104	20.8	209	12.8	127	42	372	49.3
HN-31F	GDP	54.83	1.40	14.97	10.83	0.24	1.31	2.39	0.57	1.52	0.21	11.74	100.02	430	67	133	18	14	45	5	66	13.2	204	10.7	220	24	416	7.6
HN-32F	GDP	58.26	0.96	17.68	6.60	0.14	1.59	2.40	1.83	2.54	0.17	7.96	100.13	432	71	113	20	11	28	15	105	16.7	220	12.7	120	35	421	14.6
HN-33F	GDP	54.56	1.09	16.68	7.80	0.15	2.36	2.64	1.67	2.07	0.20	11.03	100.26	401	68	250	16	11	69	7	86	15.2	211	12.0	162	34	385	36.5
HN-34F	GDP	55.07	1.50	16.98	8.54	0.21	1.83	2.56	2.00	2.65	0.20	8.55	100.09	428	132	59	17	16	18	11	116	20.7	169	17.2	184	54	832	11.8
HN-35F	GDP	56.48	1.11	17.34	8.18	0.34	1.56	2.49	2.03	3.06	0.19	7.76	100.55	506	90	90	18	12	30	18	127	15.5	179	16.4	157	40	504	3.8
HN-36F	GDP	55.33	0.99	16.65	8.25	0.17	1.71	2.55	2.01	2.61	0.25	9.89	100.42	448	82	85	17	11	25	27	106	18.2	181	13.9	155	41	447	3.6
HN-37F	GDP	56.43	1.32	15.93	8.54	0.22	1.89	2.72	2.11	2.51	0.21	8.03	99.91	418	83	195	16	13	34	13	105	16.9	201	13.2	189	40	501	8.0
HN-38F	GDP	64.05	0.75	16.30	5.56	0.23	1.46	2.49	2.92	3.24	0.08	3.13	100.21	421	80	83	18	11	16	16	146	15.0	185	24.3	100	46	385	10.3
HN-39F	GDP	63.97	1.15	14.35	8.15	0.20	1.83	2.38	2.88	2.47	0.12	2.41	99.92	391	92	1157	17	13	46	36	90	15.4	199	18.9	180	44	578	10.1
HN-40F	GDP	65.32	0.75	15.38	5.71	0.18	1.48	2.29	2.99	2.63	0.10	2.89	99.73	408	85	91	17	11	21	17	98	11.2	208	16.6	101	39	350	16.4
HN-41F	GDP	59.59	1.12	14.79	7.54	0.16	2.77	2.68	2.23	2.31	0.16	6.08	99.43	400	62	2360	18	10	107	18	86	16.4	223	9.0	178	32	340	9.6
HN-42F	GDP	52.50	0.59	18.91	5.71	0.16	1.03	1.55	2.80	2.32	0.21	14.95	100.73	363	106	47	19	12	18	5	105	13.5	140	30.1	76	58	387	38.4
HN-43F	GDP	63.49	0.90	17.23	3.78	0.24	0.62	1.12	2.93	4.92	0.06	4.34	99.64	392	180	38	18	26	17	11	202	8.3	125	57.9	60	104	584	1.9
HN-44F	GDP	61.32	1.13	15.99	7.93	0.23	1.21	2.01	3.52	2.89	0.10	3.85	100.18	360	196	86	18	18	14	8	117	12.2	165	61.9	164	77	956	9.5
HN-45F	GDP	61.10	0.63	16.41	4.90	0.15	1.24	2.03	3.84	2.62	0.08	6.95	99.95	327	114	86	17	13	26	8	104	8.7	183	30.6	72	68	431	8.7
HN-46F	GDP	62.71	1.16	14.79	7.68	0.17	1.91	2.40	2.94	2.64	0.12	3.38	99.89	382	92	1037	17	13	51	19	100	16.6	193	23.4	184	45	505	19.1
HN-47F	GDP	63.17	0.71	16.08	5.21	0.15	1.51	2.17	3.45	3.47	0.10	4.25	100.25	312	103	82	18	14	33	14	142	12.8	173	35.4	101	70	197	4.1
HN-48F	GDP	58.32	0.95	16.14	8.85	0.17	2.52	3.06	3.02	2.47	0.11	4.80	100.42	360	82	89	18	10	26	11	90	20.8	225	24.6	208	45	323	14.7
HN-49F	GDP	51.97	1.15	16.45	12.10	0.24	3.43	3.64	2.21	1.72	0.13	7.29	100.33	334	60	127	18	8	32	13	64	20.9	237	14.9	318	33	344	15.5
HN-50F	GDP	58.22	1.28	15.19	8.25	0.18	1.86	3.13	1.94	1.98	0.16	7.95	100.15	375	49	82	17	8	30	16	77	16.8	268	7.6	196	26	219	5.8
HN-51F	GDP	66.17	0.86	14.30	6.25	0.12	1.27	1.78	2.65	2.63	0.09	3.81	99.94	456	58	82	16	9	29	31	93	12.8	214	7.5	115	24	226	14.9
HN-52F	GDP	60.32	1.05	14.14	8.79	0.16	1.85	2.51	2.74	2.22	0.14	6.02	99.94	405	69	169	16	10	74	17	77	13.5	232	13.5	189	33	285	6.0
HN-53F	GDP	51.58	1.18	14.31	10.04	0.28	2.75	3.64	1.79	1.67	0.20	11.63	99.08	286	67	144	14	7	79	23	70	23.0	213	5.7	232	33	166	2.3
HN-54F	GDP	59.55	0.93	16.37	7.02	0.16	2.13	2.66	2.33	2.28	0.17	6.41	100.02	416	65	89	19	9	41	20	90	17.0	261	8.0	148	33	246	6.9
HN-55F	GDP	62.28	1.34	14.23	8.15	0.18	1.82	2.31	2.87	2.64	0.12	3.80	99.75	361	106	1207	16	16	45	14	99	13.1	181	25.8	193	49	514	23.5
HN-56F	GDP	57.46	0.82	16.65	6.58	0.25	2.35	2.44	2.67	2.71	0.13	8.11	100.17	343	92	80	18	12	37	12	109	15.5	186	26.6	126	53	225	8.1
HN-57F	GDP	64.36	0.70	14.49	4.84	0.19	1.34	1.41	2.34	2.87	0.11	7.38	100.04	411	81	102	16	11	42	19	119	8.7	150	22.0	86	38	197	9.1
HN-58F	GDP	66.95	0.73	12.32	4.92	0.23	1.34	1.08	1.13	2.00	0.11	8.51	99.31	422	64	64	13	9	42	11	92	9.7	136	7.6	86	29	194	14.2
HN-59F	GDP	62.39	0.61	15.46	6.06	0.18	1.16	1.97	2.33	2.67	0.12	7.06	100.02	506	73	81	17	8	36	12	101	10.9	206	15.9	88	32	333	5.5
HN-60F	GDP	62.08	0.60	17.19	6.74	0.25	0.92	2.30	3.92	2.53	0.09	3.90	100.52	428	114	37	19	9	14	33	87	9.6	236	35.8	98	36	649	10.5
HN-61F	DP	60.40	0.59	17.93	5.59	0.12	2.02	3.88	3.70	1.82	0.14	4.01	100.20	293	61	25	19	8	17	12	66	9.8	547	17.8	87	32	227	16.3
HN-62F	DP	57.56	1.22	15.40	11.34	0.16	2.24	3.35	3.39	1.90	0.17	3.30	100.03	309	105	55	20	12	24	13	64	11.6	415	38.0	248	43	599	13.5
HN-63F	GDP	61.16	1.95	12.92	11.30	0.28	1.91	2.41	2.67	2.57	0.10	2.29	99.57	357	118	1456	16	21	44	18	93	16.6	176	35.6	308	63	537	8.7
HN-64F	MCBDPI	62.42	0.94	14.92	6.46	0.20	1.74	2.25	2.75	2.72	0.13	5.33	99.85	384	77	610	17	11	48	20	105	14.3	185	18.0	141	38	331	6.2
HN-65F	DP	57.51	0.61	17.52	5.99	0.13	2.38	5.00	3.37	1.28	0.21	5.40	99.40	337	37	31	20	6	26	9	35	11.5	755	3.8	99	10	133	4.9
HN-66F	DP	58.97	0.58	18.41	5.69	0.10	2.47	5.29	3.77	1.21	0.18	3.06	99.73	328	35	34	21	6	26	11	29	7.7	822	2.8	92	8	128	8.5
HN-67F	DP	58.31	0.61	17.76	5.98	0.11	2.02	4.90	3.59	1.35	0.20	4.97	99.80	320	43	40	19	6	20	9	36	9.6	710	4.1	109	10	209	5.8
HN-68F	MCBDPI	63.71	1.25	14.05	7.52	0.20	1.79	2.53	2.95	2.63	0.12	2.91	99.66	372	104	986	16	15	42	23	97	15.3	206	21.0	178	51	460	7.5
HN-69F	DP	56.91	1.01	17.18	9.66	0.13	2.73	5.04	3.76	1.26	0.22	2.26	100.15	282	58	63	21	8	25	18	33	14.4	698	5.4	202	13	347	9.7
HN-70F	MCBDPI	63.24	1.24	14.15	7.90	0.18	1.84	2.65	2.72	2.53	0.12	3.26	99.83	364	91	833	16	14	38	18	92	14.4	244	19.6	191	43	406	14.0
HN-71F	DP	60.84	0.62	17.52	6.84	0.38	1.85	3.20	3.79	2.21	0.12	2.99	100.35	349	75	45	19	8	23	14	3	11.8	370	27.0	105	43	413	4.7
HN-72F	DP	60.20	0.53	18.34	5.15	0.10	2.34	5.47	4.02	1.38	0.16	1.97	99.67	310	30	23	20	6	17	13	36	9.5	797	3.2	84	10	116	10.6
HN-73F	MCBDPI	62.56	0.94	15.73	6.53	0.17	2.21	3.63	3.36	2.15	0.13	2.43	99.83	334	80	510	17	11	33	17	74	14.1	417	15.0	132	36	294	7.7
HN-74F	GDP	61.75	0.77	16.33	6.67	0.16	1.24	1.68	3.72	3.52	0.10	4.36	100.30	283	106	61	19	14	20	15	144	10.9	157	36.3	124	56	346	4.3
HN-75F	GDP	59.70	0.95	16.23	7.18	0.28	0.90	1.40	4.11	3.26	0.12	6.08	100.22	312	321	51	18	29	22	-	132	12.1	131	111.8	114	169	521	4.3
HN-76F	GDP	60.60	0.61	17.08	5.52	0.21	1.07	1.66	3.93	3.19	0.13	6.35	100.32	308	117	56	18	14	24	11	133	9.4	157	38.8	86	60	332	5.0
HN-77F	GDP	60.58	0.58	18.05	5.68	0.46	1.05	1.52	3.74	3.25	0.11	5.41	100.44	353	84	50	20	13	22	14	141	11.2	170	27.7	67	45	312	3.7
HN-78F	GDP	63.93	0.80	15.82	6.69	0.20	0.94	1.69	4.08	3.56	0.08	2.33	100.12	304	162	32	18	19	13	23	145	11.6	177	54.9	121	80	563	11.5
HN-79F	MCBDPI	58.31	1.63	14.14	12.77	0.26	2.04	3.23	3.19	2.19	0.14	1.99	99.89	316	124	708	18	18	37	13	74	15.1	351	32.2	305	58	568	4.1
HN-80F	DP	57.21	0.53	17.36	4.84	0.12	2.01	4.18	3.17	1.40	0.19	9.06	100.07	394	36	53	15	6	34	8	41	10.7	614	4.9	81	10	132	6.2
HN-81F	DP	60.07	0.52	18.07	4.98	0.10	1.98	4.91	3.71	1.39	0.18	4.02	99.92	326	34	34	19	6	17	10	36	8.9	720	3.8	76	9	134	18.0
HN-82F	DP	57.76	0.69	17.71	6.51	0.14	3.53	5.80	3.37	1.18	0.15	2.67	99.51	279	35	79	19	5	41	14	38	16.7	665	2.6	116	13	114	8.4
HN-83F	GDP	62.15	0.92	16.54	6.47	0.15	1.53	2.00	3.80	2.71	0.10	3.74	100.12	339	109	82	19	13	26	49	99	16.6	194	30.2	130	50	385	8.2
HN-84F	GDP	62.33	0.75	17.66	6.36	0.18	0.89	1.56	3.99	2.65	0.10	3.97	100.43	376	123	31	20	14	10	17	96	9.1	193	36.6	91	49	448	20.3
HN-85F	HI	65.62	0.77	15.29	6.38	0.29	0.89	1.70	3.39	2.53	0.09	3.07	100.02	371	94	38	17	13	14	20	87	10.9	193	28.7	108	43	385	8.4
HN-86F	HI	64.40	0.84	15.08	6.17	0.31	0.89	1.52	2.29	2.55	0.17	5.77	100.00	403	65	34	17	10	12	16	90	14.8	180	12.1	110	30	283	7.4
HN-87F	GDP	57.59	1.24	16.45	11.03	0.28	1.09	1.44	4.02	2.77	0.11	4.14	100.15	385	265	54	20	26	20	12	96	12.4	159	67.5	180	129	1030	4.8
HN-88F	HI	61.22	0.68	17.64	5.61	0.21	0.97	1.42	3.24	2.55	0.22	6.61	100.38	446	103	29	20	12	16	15	91	10.3	168	25.2	76	50	378	11.8
HN-89F	HI	63.43	0.91	15.31	6.70	0.17	1.05	2.90	2.08	1.62	0.17	5.62	99.97	342	61	20	19	7	7	21	52	16.4	247	9.1	132	30	250	38.9
HN-90F	HI	63.40	0.88	16.18	6.42	0.21	0.92	1.70	3.46	2.69	0.14	4.16	100.16	387	142	37	18	17	12	19	95	10.6	187	35.2	115	63	540	13.5
HN-91F	HI	62.08	1.22	16.89	5.56	0.21	0.94	1.51	2.93	2.92	0.15	5.64	100.06	410	217	20	18	20	11	37	104	14.7	179	69.0	103	88	799	9.3
HN-92F	GDP	52.17	1.72	19.86	9.69	0.17	2.17	2.74	1.85	1.25	0.17	8.45	100.23	355	76	126	23	12	49	16	50	19.0	331	12.1	214	25	554	8.3
HN-93F	HI	60.06	1.03	18.15	6.07	0.36	1.04	1.55	2.59	2.72	0.24	6.38	100.20	432	153	50	19	18	28	13	101	11.9	186	48.5	101	74	425	3.5
HN-94F	DP	56.63	0.91	17.99	7.56	0.12	3.03	5.43	3.51	1.15	0.21	3.27	99.81	287	40	38	20	7	26	12	29	14.3	794	2.7	150	11	187	6.7
HN-95F	DP	61.67	0.44	18.57	4.65	0.09	1.99	5.69	4.11	1.49	0.17	0.53	99.39	331	35	18	19	6	10	9	34	9.5	834	3.3	75	8	108	36.7
HN-96F	DP	59.04	0.59	18.06	5.27	0.10	1.86	4.08	3.06	1.52	0.21	6.23	100.03	372	44	32	19	7	20	15	46	11.0	608	5.0	85	14	138	40.5
HN-97F	DP	61.59	0.42	18.27	4.56	0.12	1.91	5.42	4.07	1.52	0.16	1.15	99.21	346	35	13	20	6	11	14	36	9.0	805	3.1	65	9	103	30.2
HN-98F	DP	55.25	0.53	16.15	4.81	0.09	1.61	3.57	2.73	1.53	0.51	13.11	99.87	338	49	44	15	7	22	9	52	9.4	497	6.6	82	17	156	38.7
HN-99F	MCBDPI	61.37	1.03	15.16	7.59	0.17	1.90	3.05	3.11	2.43	0.14	3.78	99.73	360	77	363	18	12	37	15	86	13.6	340	16.4	175	40	387	6.8
HN-100F	MCBDPI	56.04	1.28	14.41	10.96	0.22	1.97	2.65	2.53	2.11	0.21	7.51	99.89	374	90	357	18	14	50	30	78	12.2	286	21.3	254	39	399	4.2
HN-101F	DP	60.46	0.62	18.14	6.02	0.11	2.11	5.34	3.97	1.52	0.19	1.16	99.64	328	41	43	20	7	18	11	37	10.4	783	4.7	99	10	158	10.4
HN-102F	DP	60.17	0.60	17.77	5.59	0.09	2.15	5.23	3.81	1.53	0.18	1.96	99.07	321	40	26	20	7	17	11	39	9.5	765	5.3	95	12	174	28.3
HN-103F	MCBDPI	57.05	0.91	15.47	7.59	0.19	1.83	2.87	2.59	2.20	0.20	9.01	99.90	376	76	235	17	11	45	9	84	14.3	321	14.7	153	39	308	4.6

Notes: SaNr= Sample number. TYPE= Catchment type; GDP- granitoid-dominated products; DP- Daisen products; MCBDPI- main channel below Daisen products input; HI- Hata input. LOI= loss on ignition. %Fines: wt % of fines in each sample. Dash (-) = not detected.

Table 2. Major and trace element analyses of the sand fraction, Hino River (hydrous basis). Major elements wt %, trace elements ppm.

SaNr	TYPE	SiO_2	TiO_2	Al_2O_3	Fe_2O_3T	MnO	MgO	CaO	Na_2O	K_2O	P_2O_5	LOI	SUM	Ba	Ce	Cr	Ga	Nb	Ni	Pb	Rb	Sc	Sr	Th	V	Y	Zr	% Sand
HN-1S	MCBDPI	80.77	0.21	8.66	1.47	0.04	0.58	1.06	1.67	3.47	0.03	0.43	98.40	448	16	7	9	4	3	9	123	1.2	160	2.4	25	7	66	99.0
HN-2S	HI	68.18	0.31	16.13	2.47	0.10	0.63	1.43	3.40	3.58	0.09	3.47	99.79	427	29	12	18	7	5	18	131	6.0	194	6.2	18	16	87	47.5
HN-3S	GDP	71.75	0.22	15.36	1.50	0.05	0.57	1.33	3.91	3.97	0.03	0.95	99.62	372	22	1	17	6	2	15	145	4.3	189	6.4	4	13	65	94.1
HN-4S	GDP	72.25	0.68	12.11	4.09	0.09	1.34	1.60	2.38	3.37	0.06	1.28	99.25	463	41	427	14	7	37	14	122	8.1	166	6.8	86	17	124	83.1
HN-5S	GDP	77.33	0.15	11.38	1.00	0.03	0.50	0.88	2.64	4.17	0.02	0.66	98.75	377	24	39	13	5	7	182	165	1.8	96	3.5	8	4	53	87.4
HN-6S	DP	62.35	0.36	20.03	3.41	0.07	1.42	4.63	3.94	1.56	0.09	2.03	99.89	339	23	9	22	5	9	12	42	7.4	724	3.3	45	7	85	93.1
HN-7S	MCBDPI	74.30	0.30	12.61	2.25	0.06	0.88	1.95	2.68	3.35	0.05	0.67	99.09	428	23	19	13	5	10	13	119	3.9	272	5.0	29	11	97	92.4
HN-8S	B	62.61	0.53	14.89	4.64	0.10	2.46	5.99	3.45	2.07	0.14	1.85	98.73	328	36	20	18	6	16	4	58	13.9	709	3.9	68	15	97	93.5
HN-9S	B	78.41	0.15	9.85	1.10	0.03	0.56	1.09	1.96	4.20	0.02	0.88	98.25	513	11	-	10	3	2	8	144	3.9	168	2.5	11	7	68	99.9
HN-10S	GDP	72.71	0.35	13.43	3.10	0.06	0.95	1.12	1.34	3.11	0.05	3.23	99.43	540	48	94	17	7	16	22	118	6.7	187	9.7	36	17	126	90.9
HN-11S	GDP	72.10	0.30	14.09	2.37	0.05	0.57	1.05	2.03	4.57	0.03	2.25	99.40	539	33	16	17	7	4	18	176	3.6	209	8.4	27	16	111	88.8
HN-12S	GDP	72.66	0.24	14.17	2.05	0.04	0.50	0.95	2.12	4.97	0.02	1.60	99.33	547	32	5	17	7	3	18	189	5.4	193	9.7	15	15	118	95.0
HN-13S	GDP	74.59	0.42	12.23	3.15	0.08	0.58	1.10	2.18	3.49	0.03	1.44	99.29	552	40	23	15	8	2	23	134	5.6	145	8.4	43	17	135	95.7
HN-14S	GDP	73.52	0.35	12.99	2.69	0.08	0.81	1.53	2.92	3.23	0.05	1.22	99.38	560	34	28	15	5	6	16	117	5.9	155	7.0	35	16	122	76.9
HN-15S	GDP	73.27	0.40	12.34	3.08	0.06	0.79	0.90	1.29	5.04	0.04	1.76	98.96	608	34	36	14	7	6	20	209	5.8	141	7.9	34	15	136	86.8
HN-16S	GDP	70.54	0.58	13.12	4.26	0.08	1.22	1.78	2.06	4.12	0.07	1.58	99.41	533	45	332	16	7	53	18	158	12.0	189	7.2	60	20	138	88.8
HN-18S	GDP	71.11	0.62	12.59	4.46	0.08	1.47	1.18	1.82	3.72	0.04	1.97	99.07	506	28	1805	15	6	78	16	140	5.5	181	6.5	95	15	128	94.9
HN-19S	GDP	71.24	0.36	11.97	3.20	0.06	2.41	1.60	1.96	3.89	0.06	1.67	98.41	534	12	2132	13	4	166	16	135	6.1	174	3.5	43	14	109	98.0
HN-20S	GDP	71.00	0.36	13.03	3.14	0.07	1.67	1.55	2.36	3.63	0.06	1.90	98.77	538	28	1181	15	6	87	16	128	5.7	173	6.7	39	15	121	95.6
HN-21S	GDP	67.92	0.74	14.05	5.28	0.14	1.58	2.72	2.81	2.58	0.07	1.76	99.65	490	32	126	16	6	11	16	86	13.9	210	5.1	111	18	137	90.3
HN-22S	GDP	60.22	0.68	14.75	6.97	0.12	5.37	1.76	1.79	2.11	0.08	5.64	99.48	415	31	1103	18	7	339	20	70	14.8	206	6.0	122	19	138	84.6
HN-23S	GDP	64.70	1.39	11.66	10.00	0.16	2.69	1.61	1.90	2.89	0.08	1.49	98.56	443	11	5312	16	9	140	14	96	9.3	162	6.4	296	18	164	96.9
HN-24S	GDP	72.95	0.17	14.46	0.80	0.06	0.38	0.81	2.07	6.26	0.01	1.17	99.12	463	33	1	16	8	5	19	247	4.0	114	10.0	1	19	56	86.9
HN-25S	GDP	67.74	0.98	12.60	8.61	0.17	1.13	1.82	2.76	2.77	0.07	1.21	99.86	507	36	160	15	9	11	15	90	9.0	183	6.1	191	18	165	87.2
HN-26S	GDP	76.42	0.33	11.27	2.48	0.08	0.71	1.01	2.34	3.47	0.03	0.92	99.04	579	25	72	12	6	7	17	115	4.0	112	5.7	26	14	112	97.3
HN-27S	GDP	69.70	0.38	15.30	2.96	0.10	0.74	1.61	2.98	3.95	0.05	1.82	99.59	633	24	24	17	6	10	16	131	6.1	201	5.9	35	15	99	95.1
HN-28S	GDP	71.51	0.27	14.72	1.92	0.06	0.61	1.26	2.93	4.50	0.03	1.58	99.39	448	22	13	17	7	3	16	168	4.8	142	6.4	16	15	74	92.5
HN-29S	GDP	68.78	0.40	16.26	2.88	0.08	0.79	1.53	3.46	3.86	0.03	1.81	99.89	432	40	15	19	9	3	14	154	8.4	154	10.1	28	21	94	62.6
HN-30S	GDP	66.89	0.72	14.22	5.02	0.10	1.52	2.04	1.90	3.74	0.08	3.25	99.49	502	43	49	17	7	25	20	149	11.8	186	7.3	85	24	190	50.7
HN-31S	GDP	66.20	1.06	14.68	7.94	0.16	1.12	2.02	0.66	1.73	0.09	4.24	99.90	388	41	110	18	11	36	18	72	10.0	233	6.7	169	14	195	92.4
HN-32S	GDP	69.81	0.58	13.79	4.16	0.08	1.08	1.55	1.66	4.23	0.08	2.34	99.37	574	31	41	16	7	12	21	159	9.7	191	6.1	58	18	138	85.4
HN-33S	GDP	67.99	0.73	13.27	5.64	0.09	1.69	1.90	1.79	3.57	0.07	2.69	99.42	529	30	122	14	7	42	19	121	10.2	198	4.6	113	16	134	63.5
HN-34S	GDP	75.27	0.49	11.00	2.97	0.06	0.78	1.09	1.39	4.56	0.04	1.13	98.79	581	38	17	12	6	5	14	165	5.3	120	6.0	49	16	141	88.2
HN-35S	GDP	76.57	0.37	10.59	2.66	0.09	0.73	1.15	1.44	4.37	0.04	1.05	99.06	557	34	16	11	5	5	16	162	8.3	119	6.4	42	16	132	96.2
HN-36S	GDP	75.84	0.30	11.02	2.48	0.05	0.73	1.29	1.75	4.21	0.05	0.99	98.70	548	27	20	11	4	6	23	152	3.7	139	5.3	36	14	129	96.4
HN-37S	GDP	72.84	0.62	11.55	4.06	0.08	1.08	1.62	1.84	3.94	0.06	1.33	99.01	529	39	81	13	6	19	19	139	8.7	160	5.8	87	17	141	92.0
HN-38S	GDP	75.03	0.40	11.36	2.68	0.09	0.84	1.15	1.74	4.62	0.03	0.97	98.91	540	31	23	13	6	6	14	180	5.1	121	7.5	43	19	133	89.7
HN-39S	GDP	72.64	0.49	12.80	3.35	0.08	1.16	1.44	2.51	3.50	0.06	1.29	99.32	485	25	408	15	6	32	15	124	6.1	167	6.4	62	15	111	89.9
HN-40S	GDP	72.04	0.33	14.08	2.42	0.08	0.83	1.38	2.63	4.04	0.04	1.50	99.38	522	28	29	16	6	10	16	146	7.0	166	6.0	32	13	90	83.6
HN-41S	GDP	70.57	0.64	12.39	4.29	0.09	2.22	1.68	2.27	2.98	0.08	1.86	99.09	467	34	1053	14	7	93	14	102	7.8	184	6.6	95	19	134	90.4
HN-42S	GDP	76.94	0.24	10.95	1.82	0.06	0.42	0.72	2.06	4.21	0.02	1.39	98.83	460	38	4	12	7	1	14	159	1.9	94	7.2	20	15	82	61.6
HN-43S	GDP	75.05	0.15	13.29	0.77	0.04	0.32	0.39	1.38	6.53	0.01	1.28	99.21	470	17	-	14	7	3	15	272	0.0	62	5.7	-	13	59	98.1
HN-44S	GDP	73.25	0.37	13.12	2.45	0.08	0.62	0.97	2.61	4.57	0.03	1.16	99.23	457	32	31	15	7	4	15	181	5.5	115	13.0	34	17	104	90.5
HN-45S	GDP	73.39	0.27	13.53	1.87	0.07	0.60	1.02	2.91	4.33	0.02	1.27	99.27	432	35	28	16	7	6	14	169	4.4	107	8.4	18	19	74	91.3
HN-46S	GDP	73.77	0.37	12.33	2.63	0.06	0.94	1.28	2.45	3.82	0.05	1.44	99.14	465	35	92	14	6	21	16	143	5.1	146	6.0	43	15	94	80.9
HN-47S	GDP	75.51	0.24	12.01	1.72	0.06	0.62	0.98	2.71	4.34	0.04	0.77	98.98	347	35	10	13	7	8	13	181	5.1	96	11.3	18	26	76	95.9
HN-48S	GDP	70.50	0.38	13.99	3.21	0.08	1.20	1.76	3.02	3.83	0.05	1.38	99.38	453	22	23	15	6	9	13	141	6.6	179	7.1	51	16	81	85.3
HN-49S	GDP	67.97	0.60	13.36	5.80	0.11	1.97	2.48	2.49	2.92	0.06	1.79	99.55	449	29	44	14	5	16	12	100	12.3	211	5.8	121	18	95	84.5
HN-50S	GDP	66.72	0.87	14.36	5.98	0.12	1.55	2.47	2.50	2.86	0.09	2.23	99.76	464	38	24	16	7	11	27	103	15.2	247	9.0	126	22	161	94.2
HN-51S	GDP	73.10	0.48	12.72	3.12	0.07	0.91	1.27	2.88	3.06	0.06	1.76	99.42	499	40	25	14	6	11	29	109	6.5	176	7.0	45	17	144	85.1
HN-52S	GDP	71.84	0.54	12.74	3.94	0.09	1.26	1.75	2.89	2.98	0.07	1.33	99.43	453	42	41	14	6	28	18	106	7.7	192	8.1	73	19	135	94.0
HN-53S	GDP	64.79	1.00	12.64	8.42	0.22	2.46	3.05	2.27	1.89	0.12	2.38	99.25	321	42	144	15	6	51	31	71	20.4	175	9.0	196	26	133	97.7
HN-54S	GDP	71.23	0.49	13.16	3.86	0.08	1.33	2.22	2.84	2.89	0.08	1.21	99.39	460	39	29	14	6	16	16	100	8.2	224	6.4	69	18	135	93.1
HN-55S	GDP	70.56	0.57	13.36	3.75	0.08	1.25	1.66	2.66	3.55	0.06	1.84	99.33	445	31	238	15	8	31	18	134	6.5	174	7.1	69	18	119	76.5

SaNr	TYPE	SiO_2	TiO_2	Al_2O_3	Fe_2O_3T	MnO	MgO	CaO	Na_2O	K_2O	P_2O_5	LOI	SUM	Ba	Ce	Cr	Ga	Nb	Ni	Pb	Rb	Sc	Sr	Th	V	Y	Zr	%Sand
HN-56S	GDP	75.54	0.25	11.79	2.24	0.07	0.88	1.06	2.34	3.87	0.04	1.06	99.14	385	24	12	13	5	6	15	155	4.8	104	7.5	26	14	75	91.9
HN-57S	GDP	77.14	0.25	10.86	2.12	0.07	0.67	0.65	1.75	3.87	0.04	1.50	98.92	397	25	111	12	6	12	23	159	4.7	88	6.9	28	14	80	90.9
HN-58S	GDP	73.36	0.52	12.44	4.42	0.18	1.13	0.69	1.40	2.66	0.06	2.57	99.42	529	50	30	16	7	20	28	106	7.9	111	7.1	75	18	136	85.8
HN-59S	GDP	70.90	0.46	13.85	4.29	0.10	0.85	1.52	2.52	3.55	0.06	1.56	99.69	534	55	12	16	7	7	21	131	8.6	189	13.6	49	23	174	94.5
HN-60S	GDP	71.96	0.37	13.74	3.45	0.11	0.70	1.48	2.94	3.53	0.05	1.19	99.50	472	50	8	16	7	3	17	129	4.6	178	12.9	34	19	125	89.5
HN-61S	DP	67.72	0.32	15.98	3.04	0.07	1.28	3.50	3.30	3.06	0.08	0.83	99.17	337	29	8	17	5	7	13	109	7.9	530	4.5	37	10	86	83.7
HN-62S	DP	67.79	0.54	14.71	5.22	0.08	1.24	2.74	3.18	2.98	0.08	1.17	99.72	373	49	16	17	7	9	13	106	6.5	387	11.0	94	15	109	86.5
HN-63S	GDP	72.54	0.49	12.72	3.25	0.08	1.10	1.52	2.51	3.76	0.05	1.19	99.23	477	37	127	14	7	27	16	139	4.5	166	6.6	60	18	115	91.3
HN-64S	MCBDPI	77.10	0.21	11.12	1.52	0.05	0.64	0.98	2.24	4.08	0.03	0.79	98.75	482	17	38	11	4	12	14	151	4.0	121	3.8	19	11	72	93.8
HN-65S	DP	62.78	0.39	18.68	3.70	0.07	1.73	5.22	4.26	1.69	0.11	0.73	99.35	367	33	10	21	6	10	11	40	8.1	823	4.1	49	8	97	95.1
HN-66S	DP	63.89	0.43	17.81	3.99	0.07	1.83	4.77	4.17	1.86	0.12	0.64	99.57	397	30	12	20	6	12	11	48	7.6	750	4.4	59	9	108	91.5
HN-67S	DP	63.75	0.43	17.79	4.12	0.08	1.75	4.82	4.15	1.70	0.10	0.73	99.41	360	27	9	20	6	10	11	43	9.2	713	2.8	59	8	101	94.2
HN-68S	MCBDPI	74.11	0.33	12.46	2.37	0.06	0.95	1.42	2.58	3.75	0.05	1.08	99.18	478	30	66	13	5	19	16	137	7.7	166	4.9	32	14	98	92.5
HN-69S	DP	63.29	0.39	18.76	3.96	0.07	1.69	5.25	4.37	1.51	0.11	0.66	100.06	318	32	11	21	5	10	11	40	6.9	795	3.4	60	9	85	90.3
HN-70S	MCBDPI	71.10	0.49	13.45	3.48	0.07	1.16	1.75	2.74	3.55	0.06	1.53	99.37	452	32	77	15	6	24	18	132	7.8	205	6.2	66	16	113	86.0
HN-71S	DP	72.10	0.27	14.07	2.50	0.14	0.78	1.72	3.29	3.48	0.04	0.96	99.35	425	34	4	15	6	6	12	128	3.6	228	8.0	28	14	86	95.3
HN-72S	DP	62.80	0.37	18.73	3.54	0.07	1.74	5.33	4.28	1.65	0.09	0.69	99.29	347	32	6	20	5	9	12	41	10.1	812	3.2	50	9	90	89.4
HN-73S	MCBDPI	72.32	0.34	13.51	2.48	0.06	1.01	1.80	2.71	3.67	0.05	1.18	99.14	468	30	47	14	5	19	17	133	5.6	237	5.1	37	12	96	92.3
HN-74S	GDP	77.31	0.21	11.45	1.49	0.05	0.46	0.65	2.59	4.17	0.02	0.68	99.10	317	27	3	12	7	3	11	180	2.6	84	13.2	14	15	68	95.7
HN-75S	GDP	75.17	0.18	12.62	1.21	0.06	0.36	0.58	2.79	5.14	0.02	0.77	98.89	411	19	3	14	7	2	18	212	1.8	67	8.7	10	21	62	95.7
HN-76S	GDP	77.68	0.17	11.25	1.13	0.05	0.35	0.57	2.50	4.51	0.02	0.61	98.84	379	22	-	12	6	2	12	191	1.6	75	7.2	9	16	60	95.0
HN-77S	GDP	76.00	0.13	12.34	1.13	0.12	0.37	0.62	2.58	4.96	0.02	0.69	98.97	427	6	-	13	5	3	13	206	2.6	97	4.2	1	10	50	96.3
HN-78S	GDP	75.48	0.18	12.68	1.23	0.06	0.43	0.89	2.95	4.44	0.02	0.68	99.04	351	20	1	14	6	2	13	186	2.7	120	7.1	2	15	62	88.5
HN-79S	MCBDPI	74.71	0.72	10.76	4.29	0.13	0.80	1.36	2.30	3.46	0.05	0.55	99.13	405	60	114	13	12	11	14	131	8.0	158	10.4	107	31	139	95.9
HN-80S	DP	63.66	0.41	17.96	3.80	0.07	1.82	4.70	4.05	1.74	0.08	0.96	99.25	395	26	15	19	5	10	12	43	8.5	704	3.4	52	6	95	93.8
HN-81S	DP	63.60	0.41	17.59	4.06	0.08	1.79	4.83	4.05	1.71	0.11	0.75	98.98	358	30	11	20	6	11	18	41	9.1	710	3.9	59	8	96	82.0
HN-82S	DP	61.93	0.39	18.82	3.77	0.08	1.95	5.47	4.13	1.42	0.08	0.89	98.92	303	25	34	21	5	18	16	40	10.7	777	2.5	57	8	81	91.6
HN-83S	GDP	73.78	0.25	13.47	1.65	0.05	0.61	0.97	3.50	3.84	0.03	0.87	99.03	436	32	8	16	6	5	20	142	3.5	125	8.9	14	15	85	91.8
HN-84S	GDP	73.02	0.23	14.18	1.70	0.07	0.48	1.19	3.53	3.80	0.03	1.14	99.38	424	22	6	16	7	2	15	135	1.4	159	6.6	14	13	67	79.7
HN-85S	HI	75.83	0.23	12.51	1.51	0.09	0.42	0.98	3.10	3.84	0.02	0.68	99.20	460	26	3	14	6	2	15	134	3.4	144	7.8	12	14	76	91.6
HN-86S	HI	75.75	0.25	11.72	2.24	0.10	0.42	0.80	2.42	3.87	0.05	1.33	98.96	473	15	-	12	5	1	14	141	3.9	140	6.0	21	13	80	92.6
HN-87S	GDP	72.39	0.24	14.55	1.61	0.08	0.48	0.80	3.65	4.75	0.02	0.87	99.43	487	28	1	17	7	2	18	174	3.1	112	8.7	9	16	83	95.2
HN-88S	HI	75.67	0.19	12.29	1.64	0.06	0.34	0.70	2.78	4.43	0.04	1.00	99.14	529	20	-	14	5	0	16	153	1.1	107	5.6	7	12	68	88.2
HN-89S	HI	69.12	0.60	13.81	4.22	0.11	0.78	2.10	2.24	2.17	0.10	4.31	99.58	359	32	10	16	6	3	18	72	11.8	231	5.0	78	21	125	61.1
HN-90S	HI	74.73	0.41	12.73	1.90	0.08	0.41	1.00	3.12	3.83	0.03	0.95	99.20	430	41	2	14	11	5	16	135	5.1	141	7.7	21	19	99	86.5
HN-91S	HI	75.11	0.62	12.47	1.75	0.08	0.38	1.01	2.67	4.08	0.03	0.88	99.07	416	38	1	14	15	2	19	146	2.4	151	10.9	35	32	118	90.7
HN-92S	GDP	63.26	0.34	20.41	3.38	0.06	0.80	3.35	3.04	1.84	0.08	3.67	100.23	334	21	31	21	4	19	13	60	5.0	557	3.8	47	9	72	91.7
HN-93S	HI	74.95	0.17	13.21	1.17	0.07	0.34	1.23	2.67	4.46	0.04	0.90	99.21	406	18	1	13	6	2	16	163	1.7	201	3.4	5	12	53	96.5
HN-94S	DP	61.52	0.43	19.68	3.87	0.07	1.88	5.80	4.43	1.40	0.09	0.73	99.89	291	33	14	21	5	13	11	34	9.0	901	2.9	56	8	89	93.3
HN-95S	DP	63.60	0.38	18.08	3.79	0.08	1.76	5.24	4.32	1.68	0.11	0.30	99.35	349	27	13	20	5	8	9	40	9.5	787	3.5	46	8	90	63.3
HN-96S	DP	63.36	0.49	17.26	4.88	0.08	1.96	4.42	3.83	1.88	0.13	1.52	99.80	389	29	19	19	6	12	92	48	10.5	659	5.3	67	10	107	59.5
HN-97S	DP	63.55	0.38	18.02	3.86	0.10	1.78	5.16	4.28	1.70	0.11	0.35	99.29	352	28	16	19	6	9	9	41	9.2	779	3.7	51	8	89	69.8
HN-98S	DP	67.71	0.35	14.75	3.12	0.06	1.39	3.34	3.23	2.46	0.09	1.85	98.35	394	24	10	16	5	10	11	74	5.7	521	4.4	45	9	85	61.3
HN-99S	MCBDPI	74.53	0.45	11.51	3.40	0.07	0.88	1.85	2.30	3.24	0.05	0.66	98.96	431	33	33	13	6	8	12	114	6.1	252	4.7	80	13	105	93.2
HN-100S	MCBDPI	76.33	0.39	10.58	3.14	0.07	0.82	1.62	2.12	3.29	0.05	0.45	98.87	448	29	18	11	6	5	12	114	5.4	230	4.7	58	10	97	95.8
HN-101S	DP	63.96	0.50	17.01	5.11	0.09	1.95	4.74	3.98	1.84	0.13	0.39	99.70	371	29	18	19	6	13	9	46	10.7	688	4.3	85	10	98	89.6
HN-102S	DP	64.92	0.39	17.16	3.73	0.07	1.72	4.71	3.85	1.93	0.10	0.64	99.22	354	28	15	18	5	10	13	51	9.1	712	3.9	51	9	86	71.7
HN-103S	MCBDPI	78.98	0.21	9.89	1.65	0.04	0.63	1.29	1.80	3.53	0.04	0.36	98.42	453	20	6	10	4	5	12	124	3.1	189	3.7	28	7	69	95.4

Notes: SaNr= Sample number. TYPE= Catchment type; GDP- granitoid-dominated products; DP- Daisen products; MCBDPI- main channel below Daisen products input; HI- Hata input; B- beach samples. LOI= loss on ignition. %Sand: wt % of sand in each sample. Dash (-) = not detected.

Table 3. Summary statistics for all <180μm and sand fraction samples (anhydrous normalized data).

	Fine Fraction N= 101				***Sand Fraction*** N= 102			
Element	Mean	Min	Max	SDp	Mean	Min	Max	SDp
Major elements (wt%)								
SiO_2	63.55	52.22	73.74	3.59	72.60	62.04	82.45	4.88
TiO_2	0.98	0.36	3.18	0.42	0.43	0.13	1.43	0.22
Al_2O_3	17.14	12.13	22.05	1.75	14.04	8.84	21.14	2.46
Fe_2O_3T	7.52	2.06	22.02	2.84	3.35	0.79	10.30	1.74
MnO	0.20	0.09	0.48	0.08	0.08	0.03	0.22	0.03
MgO	1.94	0.62	9.57	1.10	1.13	0.33	5.72	0.74
CaO	2.89	1.18	5.99	1.23	2.06	0.40	6.18	1.47
Na_2O	3.09	0.65	4.82	0.81	2.76	0.69	4.47	0.83
K_2O	2.54	1.19	5.16	0.76	3.50	1.41	6.67	1.09
P_2O_5	0.15	0.04	0.58	0.07	0.06	0.01	0.14	0.03
Trace elements (ppm)								
Ba	396.5	287.9	574.8	63.9	456.0	293.6	647.5	77.8
Ce	91.8	10.7	340.8	49.5	31.1	6.0	61.0	9.6
Cr	493.7	13.4	8487.9	1234.1	179.6	0.4	5471.7	645.0
Ga	19.0	12.5	24.7	1.9	15.7	9.5	22.3	2.8
Nb	12.4	5.5	30.9	4.8	6.4	3.1	15.6	1.7
Ni	48.2	7.5	743.5	86.6	20.1	0.7	361.3	43.0
Pb	20.7	5.2	418.2	40.4	18.4	3.9	185.2	18.8
Rb	94.4	3.5	212.3	37.7	126.7	34.1	277.3	49.9
Sc	14.2	5.8	26.3	4.1	6.8	0.05	21.0	3.6
Sr	313.1	118.6	850.0	204.3	272.7	63.3	908.9	227.8
Th	21.9	2.7	118.8	18.7	6.6	2.5	13.9	2.5
V	149.7	33.4	696.0	88.4	53.8	0.5	304.8	46.1
Y	42.8	8.3	179.1	26.3	15.2	3.8	32.7	5.2
Zr	406.5	105.5	1072.7	203.0	106.2	50.4	203.5	31.9

Min Minimum
Max Maximum
SDp Population standard deviation

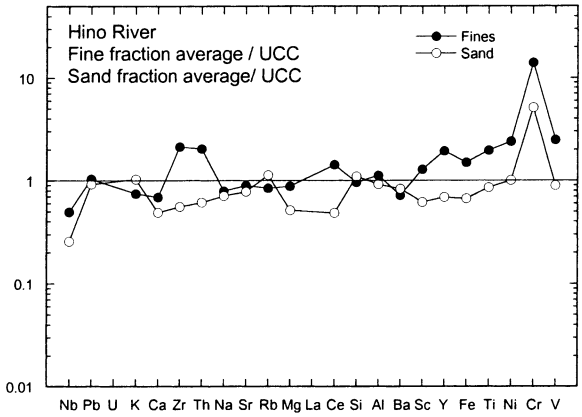

Fig. 2. Multi-element plot showing the average composition (anhydrous normalized) of the fine (<180μm) and sand fractions from the Hino River (data from Tables 1 and 2) normalized against the Upper Continental Crust (UCC) average of Taylor and McLennan (1985). Elements are arranged from left to right in order of increasing normalized abundance in average Mesozoic-Cenozoic greywacke (Condie, 1993) relative to UCC, following the methodology of Dinelli *et al.,* (1999). The major elements are normalized as oxides.

given in Table 3, calculated from analyses normalized to 100% to negate the effects of varying LOI. Average elemental abundances show considerable contrast between the fractions, especially for some trace elements (e.g. Cr, Zr). The average compositions of both fractions over the entire suite broadly correspond with that of average Upper Continental Crust (UCC), although some differences are also evident (Fig. 2). The fine fraction is slightly depleted in Nb, K, Ca and Ba with respect to UCC, whereas Zr, Th, and Ce abundances are a little greater. The greatest divergence from UCC in the fine fraction average is observed in the segment Sc-V, where all elements are progressively enriched, with a marked peak in Cr of more than 10 times UCC abundance. All of this group of elements are associated with mafic components. The pattern for the fine fraction average is generally linear, and is inclined from left to right, similar to the composition of average Mesozoic-Cenozoic greywacke (Condie, 1993; Dinnelli *et al.,* 1999). In contrast, the pattern of the sand fraction average is almost flat, and most elements are slightly depleted compared to UCC, especially for Nb, Ca-Sr, and Mg-Ce. Abundances also tend to increase in the segment Sc-V, as in the fine fraction, but generally remain less than or equal to UCC levels. Only the content of Cr is significantly enriched relative to UCC, although to a lesser degree than in the fine fraction.

Combined histograms (bar charts) of anhydrous-normalized elements for the fine and sand fractions display clear dependence on grain size, although overlap is considerable. The fine fractions tend to have greater abundances of most elements, except for SiO_2, K_2O, and to a lesser extent Ba, Pb, and Rb, which are enriched in the sand fraction (Fig. 3 and 4). Na_2O (Fig. 3), Sr, and Pb show relatively little contrast in the ranges of their distributions in the fractions. However, statistical tests suggest that the means of all elements except Sr and Pb differ significantly (95% confidence level) between the two fractions.

Fine Fraction

Most of the major elements have variable distributions and contain anomalous values. Distribution of SiO_2 (Fig. 3a) is relatively normal except for lower values in several samples, coupled with higher abundances of other elements. This is especially marked in sample HN 23, which has the lowest SiO_2 content (52.2%) due to enrichment in Fe_2O_3 (22.02%), TiO_2 (3.18%), and MnO (0.38%), probably as a result of Fe-Ti-Mn oxide heavy mineral concentration or authigenic Fe-Mn-O crust material. TiO_2 (Fig. 3b), Fe_2O_3T and MnO are markedly skewed to higher values. MnO and P_2O_5 show the same characteristic, but to a lesser extent. The remaining distributions are more irregular, with K_2O (Fig. 3c) and Na_2O (Fig. 3d) possibly bimodal, whereas Al_2O_3 and CaO are polymodal.

Trace elements have also variable abundances. Ba (Fig. 4a) and Ga resemble normal distributions, with few anomalous values. Cr (Fig. 4b), Ce, Ni, Pb, Th, V, and Y are strongly skewed to higher values, with some of the most anomalous values recorded in sample HN 23 (e.g. Cr 6629 ppm; V 696 ppm; Zr 578 ppm). Several other samples also have extreme values, such as HN 17 (Cr 8488 ppm; Ni 744 ppm), HN 87 (Zr 1073 ppm), and HN 25 (Zr 1048 ppm). The distribution of Sr (Fig. 4c) is clearly bimodal, with a marked contrast between one group with relatively low values (100 to 400 ppm) and another with high values (500-900 ppm). The latter group is associated with samples collected from streams draining Mount Daisen. The

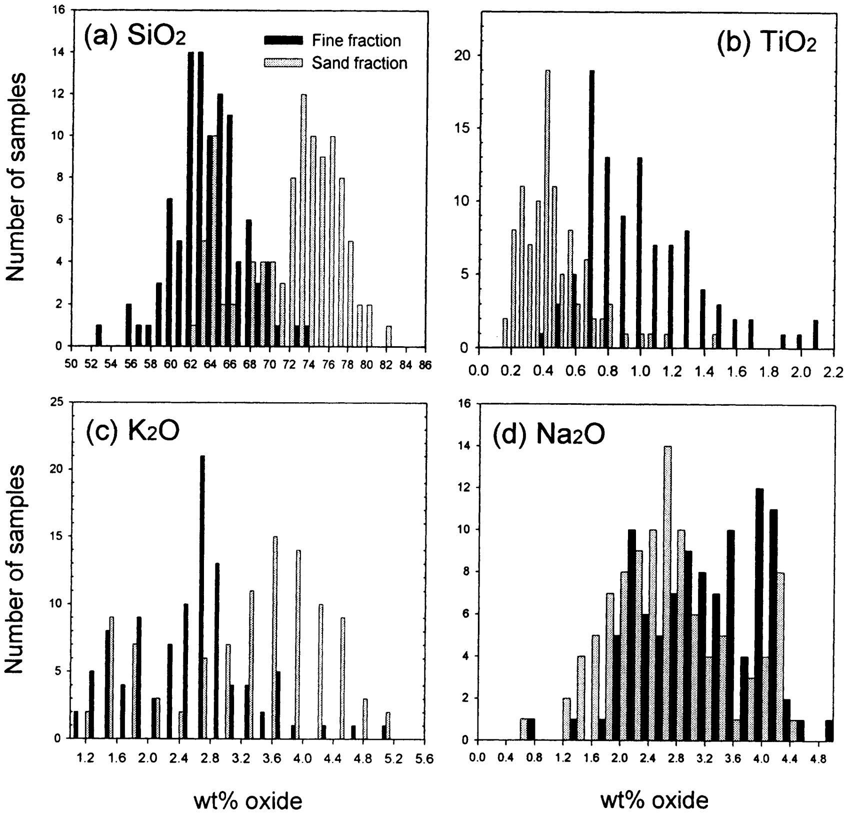

Fig. 3. Examples of combined histograms of major element abundances (anhydrous normalized data) in the <180μm and sand fractions, Hino River. (a) SiO_2 - normal distribution; (b) TiO_2 - skewed to higher values; one sample with >2.2 wt% not plotted; (c) K_2O - bimodal, two samples >5.6 wt% not plotted; (d) Na_2O - distinctly polymodal.

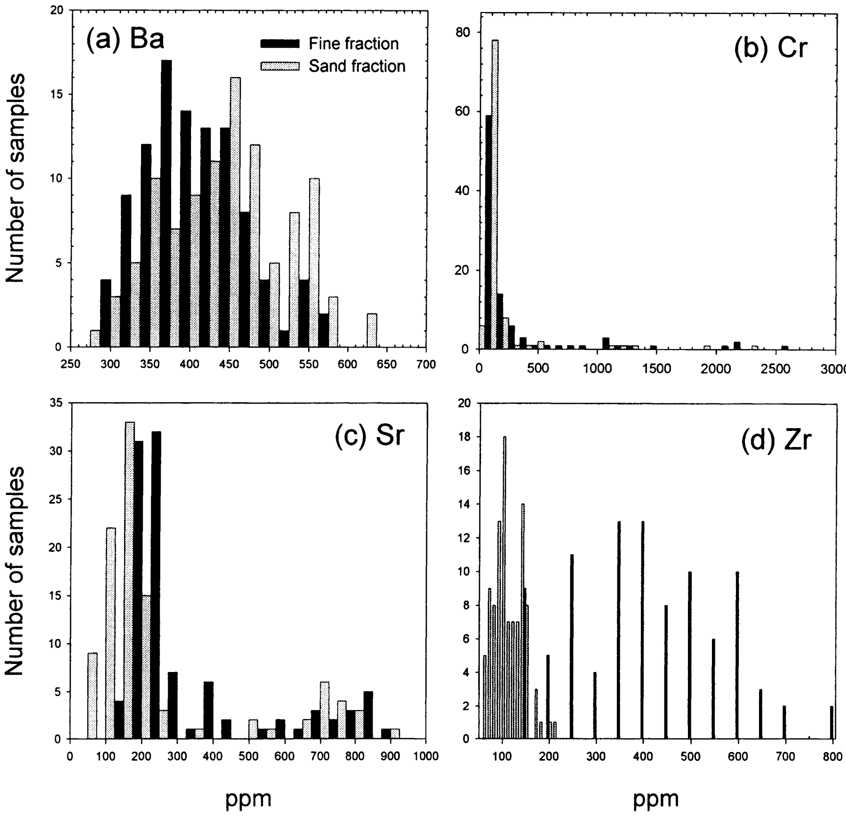

Fig. 4. Examples of combined histograms of trace element abundances (anhydrous normalized data) in the <180μm and sand fractions, Hino River. (a) Ba - normal distribution; (b) Cr - strongly skewed to higher values, five samples with 3400-8500 ppm not plotted; (c) Sr - clear bimodal distributions and (d) Zr - polymodal, five samples with 845-1080 ppm not plotted.

remaining trace elements analyzed (Zr (Fig. 4d), Nb, Rb, and Sc) have comparatively wide ranges and polymodal distributions.

Sand fraction

The most notable feature of the patterns among the major elements is the relatively high number of bimodal distributions (five in total), all of which identify a group of samples from streams that drain catchments consisting almost exclusively of products from Mount Daisen. For SiO_2 (Fig. 3a) and K_2O (Fig. 3c) this mode is found at lower values, whereas for Na_2O (Fig. 3d), Al_2O_3, and CaO it occurs at higher values. In all cases, contrast between the two major modes is evident, and reflects the strong geochemical signature that volcanic products from Mount Daisen imprint to the sediments. The remaining major elements (TiO_2 (Fig. 3b), Fe_2O_3, MnO, MgO, and P_2O_5) exhibit variable and strongly right-skewed distributions. As in the fine fraction, several samples have lower SiO_2 values due to enrichment in Fe_2O_3, TiO_2, and MnO, and again this is most marked in sample HN 23.

Among the trace elements, a number of elements (Ba (Fig. 4a), Ce, Ga, and Sc) have normal distributions with relatively few anomalous values. In contrast Cr (Fig. 4b), Nb, Ni, Pb, and V are moderately to strongly skewed to higher values. Sr (Fig. 4c), Rb and to a lesser extent Y display bimodal distributions, with one of the modes associated with Daisen products. The contrast between the modes is particularly marked for Sr. Finally, abundances of Zr (Fig. 4d) and Th vary considerably, and distributions are polymodal.

Anomalous values

Elemental abundances in both fractions generally have positively skewed distributions. Most of the elements analyzed are not prone to disturbance from human activity, but several elements have elevated values (>2 s.d.) that could be considered exceptional. Anomalous values are most commonly observed for Cr, from samples (e.g., HN 17 -20, 22, 23) containing basic and ultrabasic rocks in their catchments. These values may have been increased by activity related to chromium mining in the area. Some of this group of samples also contain elevated levels of Ni. With one exception, abundances of the potentially environmentally sensitive element P_2O_5, are low and within the range expected for the source lithotypes. There is thus no clear evidence in the sediments for anthropogenic inputs (e.g. via fertilizers). The compositions observed suggest clear association with the characteristics of source rock lithotypes and derived products. Greater values for a group of elements including Fe, Mn, Ti, Cr, Ni, Ce, Th, V, Y, and Zr are very likely related to concentrations of high density accessory minerals (see Ortiz & Roser, 2003). This will be verified by future work.

The bimodal and polymodal distributions observed reflect the control of rock source in the composition of derived sediments. As already stated, this is particularly distinctive in the sand fraction, including the bimodal patterns of SiO_2, K_2O, Al_2O_3, CaO, Na_2O, and Sr, elements for which one of the modes is clearly associated with samples collected from catchments draining Mount Daisen.

Classification of sample sites by source categories

As described above, the geology of the Hino river catchment differs spatially, with felsic igneous and volcanic rocks dominating the central and southern parts, volcanic products from Mount Daisen in the northeast, and volcanic rocks of the Hata Formation in the northwest. Following the methodology adopted by Ortiz and Roser (2003) for the Kando River, sample localities from the Hino watershed were divided into four categories according to the characteristics of their main source rocks. The sand fractions include an additional category consisting of two samples (HN 8, 9) collected from the beach in Miho Bay. The <180 μm fraction in these two samples was too small to be analyzed.

The main categories are:

(1). Granitoid-dominated products (GDP) and felsic volcanics, covering a vast area and including more than 61% of the total sample sites;
(2). Daisen products (DP), consisting of samples from catchments dominated by volcanic products from Mount Daisen, although sites HN 61, 62, 69, and 71 also contain other lithologies (e.g., granitoids, psammitic schists);
(3). Main channel below Daisen product input (MCBDPI); namely HN 1, 7, 64, 68, 70, 73, 79, 99, 100, and 103;
(4). Hata Formation input (HI); sites HN 2, 85, 86, 88, 89, 90, 91, and 93.

Simple element-Al_2O_3 variation diagrams constitute a useful tool to illustrate differences between abundances of elements according to the above categories. The first feature observed is that although there is significant overlap and scatter, the distributions of elements show broad linear trends from the sand fractions (concentrated at lower abundances of Al_2O_3) toward the fine fraction. These linear trends are especially clear for SiO_2 (Fig. 5) and Ga (Fig. 6). Distribution of the fractions with respect to Al_2O_3 corresponds with the histograms of elemental abundances (Figs. 3 and 4), and illustrate the dependence of chemical composition on grain size as reported by several authors (e.g., Fralick & Kronberg, 1997; Vital & Stattegger, 2000).

The distributions of the major elements generally overlap, but samples derived from Daisen products tend to be distinguishable. This is especially clear for CaO (Fig. 5b), and K_2O (Fig. 5c), for which samples in both fractions from that category have higher and lower values (respectively) compared to the other categories. Fe_2O_3 (Fig. 5d), TiO_2, and MnO abundances in the fine fractions tend to be greater

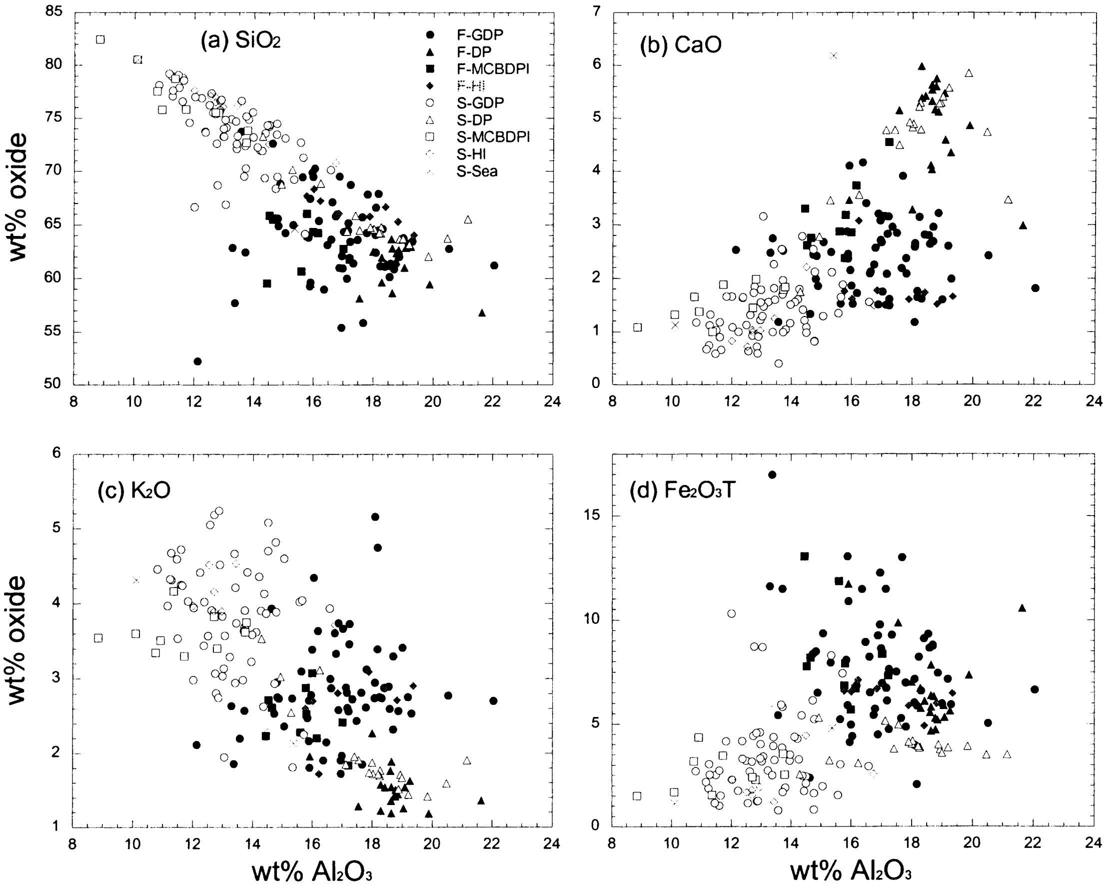

Fig. 5. Examples of major element-Al_2O_3 variations in the fine and sand fractions (anhydrous normalized data), Hino River, according to main source lithotypes. F - <180 μm (fine) fraction; S - sand fraction; - GDP = granitoid-dominated, - DP= Daisen products; - MCBDPI = main channel below Daisen product input - HI= Hata input; - sea = beach sands. (a) SiO_2 - linear trend between sand and fine fractions, lower abundances in samples derived from Daisen products; (b) CaO - greater abundances in samples from Daisen products; (c) K_2O - lower abundances in samples from Daisen products, two samples with >6 wt% not plotted; and (d) Fe_2O_3T - abundances in the fine fractions greater than the sands in each category, one sample with >18 wt% not plotted.

than the sands in each category. Conversely, for Na_2O, MgO, and P_2O_5 only sand fractions derived from Daisen products have distinctively higher values, whereas for SiO_2 (Fig.5a) the same samples have lower values. Samples derived from Hata Formation rocks generally show little contrast with samples from granitoid-dominated sites, and tend to plot towards lower values only for CaO (Fig. 5b) and MgO, especially the fine fraction. Although scatter is considerable, samples from the main channel below Daisen product input tend to have values intermediate between Daisen products and the granitoid-dominated group, reflecting mixing of detritus in the lower reaches of the river. Beach sample HN 8, collected from the eastern part of Miho Bay, has high CaO (Fig. 5b) in its sand fraction, possibly reflecting abundance of Daisen detritus at that site.

Trace elements behave in a similar way to the major elements; and hence the most distinctive features are related to the distribution of samples derived from Daisen products. Both fractions of samples from this category plot well apart from the remaining groups, especially for Sr (Fig. 6a), with higher values; and for Y (Fig. 6b), Rb, Th, and to a lesser extent Ba and Pb, all of which have lower values than the other groups. The higher values for Sr and lower for Y reflect the adakitic nature of the Daisen volcanic products, as described in a number of studies (e.g., Morris, 1995; Kimura *et al.,* 2003). For Cr (Fig. 6c), Ce, Nb, Zr, and to a lesser extent for V, only the fine fractions of samples derived from Daisen products have distinctive lower values. Daisen-derived sand fractions overlap with the remaining categories. Conversely, for Ga (Fig. 6d) and to some degree for Sc, the Daisen sand fractions tend to have higher values, and equivalent fine fractions show little contrast with the other categories. Samples derived from Hata sources are again scattered among the granitoid-dominated data, except for Cr (Fig. 6c) and Ni, for which concentrations tend to be lower in the fine fractions. This suggests the geochemical signatures of Hata inputs do not differ greatly from those derived from granitoid-dominated catchments.

Although overlap and scatter are significant, trace element abundances in samples from the lower main

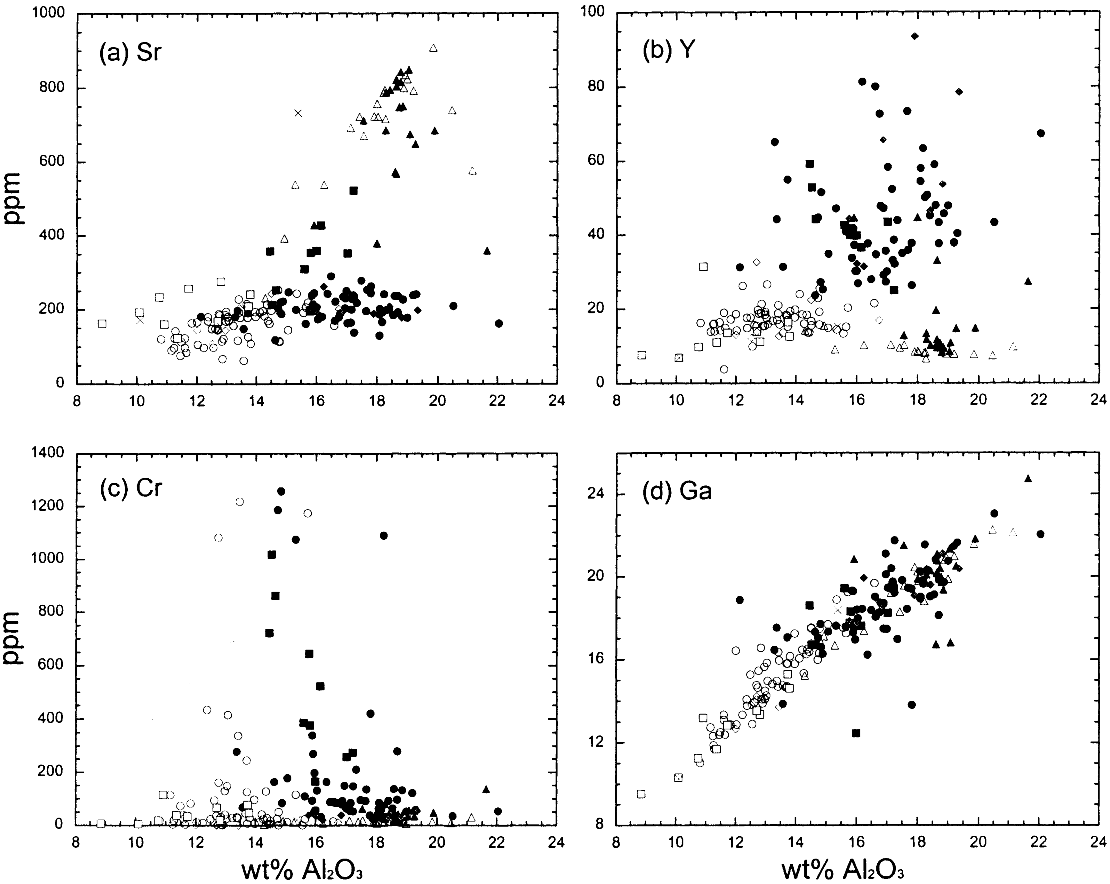

Fig. 6. Examples of trace element-Al_2O_3 variations in the fine and sand fractions (anhydrous normalized data), Hino River, according to main source lithotypes. Symbols as in Fig. 5. (a) Sr - markedly greater abundances in samples form Daisen products; (b) Y - lower abundances in samples from Daisen products, four samples with >100 ppm offscale; (c) Cr - extreme abundances in some samples; 12 samples with >1400 ppm offscale (d) Ga - linear trend between fine and sand fractions.

channel tend to be intermediate between those of the granitoid- and Daisen-derived products. This represents mixing in the lower reaches of the main channel of Hino River of detritus originating from these two contrasting areas, the largest of which is mainly felsic in composition. Consequently, the primary source signatures of these two sources are obscured.

Abundances of Cr in the upper main channel are greater than those in the secondary drainages in all categories, excepting sites directly draining ultrabasic rocks (16, 17, 19). Levels in the main channel decrease relatively regularly downstream, reflecting dilution of Cr-rich detritus from the ultrabasics with Cr-poor detritus from all other lithotypes. This is most marked for the <180μm fraction, but is also evident in the sands.

Conclusions

The chemical compositions of sediments from the Hino River system are representative of the nature of their source lithotypes. Dependence of composition on grain size is displayed by contrasting elemental distributions of the <180 μm and sand fractions. The distributions reflect the influence of different lithotypes, with especially distinctive contrasts produced in sediments mainly derived from Mount Daisen. Sediments originating from Daisen record adakitic signatures from such products. Elevated concentrations for a number of elements (e.g. Zr, Cr) are likely related to local concentrations of heavy minerals. The intermediate chemistry of sediments collected from the main channel below the first input of Daisen products reflects mixing and homogenization of detritus in the lower reaches of the Hino River.

Acknowledgements

Our thanks to Takao Tokuoka for suggesting the project, to Kaoru Yamamoto for her invaluable assistance during fieldwork, and to Yoshihiro Sawada for access to the XRF.

References

Condie, K. C., 1993, Chemical composition and evolution of the upper continental crust: Contrasting results from surface samples and shales. *Chem. Geol*., **104**, 1-37.

Dinelli, E.; Lucchini, F.; Mordenti, A. and Paganelli, L., 1999, Geochemistry of Oligocene-Miocene sandstones of the northern Apennines (Italy) and evolution of chemical features in relation to provenance changes. *Sed. Geol.,* **127**, 193-207.

Editorial Board of Geological Map of Shimane Prefecture (EBGMSP), 1997, Geological map of Shimane Prefecture (1:200,000).

Fralick, P.W. and Kronberg, B.I., 1997, Geochemical discrimination of clastic sedimentary rock sources. *Sed. Geol.,* **113**, 111-124.

Hashimoto, M., 1973, Barroisites from the Sangun Metamorphic Terrane of the Nichinan-cho district, Southwest Japan. *Jour. Japanese Assoc. Mineral. Petrol. Econ. Geol.*, **68**, 177-182.

Hashimoto, M., 1990, Additional mineral data from the Sangun metamorphic rocks, Nichinan-cho district, Tottori Prefecture. *Jour. Japanese Assoc. Mineral. Petrol. Econ. Geol.*, **85**, 37-42.

Hattori, H. and Katada, M., 1964, *Explanatory text of the geological map of Japan at scale 1:50.000, Neu (Okayama-29).* Kawasaki city, Geological Survey of Japan.*

Hattori, H. and Shibata, K., 1974, Concordant K-Ar and Rb-Sr ages of the Tottori Granite, Western Japan. *Bull. Geol. Surv. Japan*, **25**, 157-173.

Iizumi, S., Mishima, H., Okamoto, Y. and Honma, H., 1984, A strontium isotope study on the Neu granitic pluton and its mafic inclusion, San'in zone, Southwest Japan. *Jour. Japanese Assoc. Mineral. Petrol. Econ. Geol.*, **79** (3), 89-100.

Iizumi, S., Imaoka, T., and Kagami, H., 2000, Sr-Nd isotope ratios of gabbroic and dioritic rocks in a Cretaceous-Paleogene granite terrain, Southwest Japan. *The Island Arc,* **9**, 113-127.

Japan Institute of Construction Engineering ("JICE"), 1984, Geological map of the Chugoku area No 3.

Kimura, J.-I. and Yamada, Y., 1996, Evaluation of major and trace element analyses using a flux to sample ratio of two to one glass beads. *Jour. Mineral. Petrol. Econ. Geol.*, **91**, 62-72.

Kimura, J.I., Okada, S., Nakayama, K., *et al.,* 1999, Fission Track ages of tephras from Daisen and Sambe volcanoes and their volcanological implications. *Quaternary Res. (Japan),* **38**, 145-155.

Kimura, J.I., Kunikiyo, T., Osaka, I., *et al.,* 2003, Late Cenozoic activity in the Chugoku area. Southwest Japan arc during back-arc basin opening and reinitiation of subduction. *The Island Arc,* **12**, 22-45.

Morris, P., 1995, Slab melting as an explanation of Quaternary volcanism and aseismicity in southwest Japan. *Geology*, **23**, 395-398.

Miura, K., Ikehara, K., and Yoshikawa, K., 1991, Volcanic ashes derived from Daisen volcano in the subsurface deposits of Japan sea, off the coast of Hokuriku region. Studies of the San'in Region, *Natural Environment*, 7-22.

Murakami, N., 1974, Some problems concerning late Mesozoic to early Tertiary igneous activity in the Inner side of Southwest Japan. *Pacific Geol.*, **8**, 139-151.

Nagao, T., Fujibayashi, N., Kagami, H., Tazaki, K., and Takata, S., 1990, Origin of the Sr-rich alkali basalts in Yokota area, Chugoku Mountains, southwest Japan. *Jour. Geol. Soc. Japan*, **96**, 795-803.*

Ortiz, E., and Roser, B.P., 2003, Major and trace element abundances in the <180 μm fractions of stream sediments from the Kando River, Shimane Prefecture, Japan. *Geosci. Rep. Shimane Univ.,* **22**, 111-120.

Ortiz, E., and Roser, B.P., 2004, Major and trace element abundances in the sand fractions of stream sediments from the Kando River, Shimane Prefecture, Japan. *Geosci. Rep. Shimane Univ.,* **23**, (this volume).

Ota, R., 1959, *Explanatory text of the geological map of Japan at scale 1: 50.000, Akasaki and Daisen (Okayama-9, 19)*. Kawasaki City, Geological Survey of Japan.*

Ota, R., 1962, *Explanatory text of the geological map of Japan at scale 1: 50.000, Yonago (Okayama-18)*. Kawasaki City, Geological Survey of Japan.*

Research Group for the Batholith in the San'in Zone, 1982, The New Granitic pluton-Petrographical study on the Batholith in the San'in Zone, Southwest Japan (part 1). *Jour. Geol. Soc. Japan*, 88, 299-310.*

Roser, B.P., Kimura, J.-I., and Hisatomi, K., 2000, Whole-rock elemental abundances in sandstones and mudrocks from the Tanabe Group, Kii Peninsula, Japan. *Geosci. Rep. Shimane Univ.*, **19**, 101-112.

Roser, B.P., Tateishi, Y., and Nakayama, K., 2001, Whole-rock geochemical compositions of Miocene sedimentary and volcanic rocks from the Izumo−Matsue districts and Shimane Peninsula, SW Japan *Geosci. Rep. Shimane Univ.,* **20**, 69-82.

Taylor, S.R., and McLennan, S.M., 1985, *The continental crust: its composition and evolution*. Blackwell Scientific, Oxford, 312 p.

Vital, H. and Stattegger, K., 2000, Major and trace elements of stream sediments from the lowermost Amazon River. *Chem. Geol.,* **168**, 151-168.

*In Japanese, English abstract or summary
(Received: Oct. 14, 2004, Accepted: Nov. 28, 2004)

（要　旨）

E. Ortiz・B.P. Roser, 2004，鳥取県，日野川の河川堆積物の 180 μm 以下と砂部分の堆積物の主成分ならびに微量成分組成．島根大学地球資源環境学報告，23，27-37

鳥取県，日野川の現河床から採取した 103 の試料を 180 μm より細粒な堆積物と砂部分に分け，それぞれについて XRF 分析による主成分元素と 14 の微量成分元素の解析を行った．元素含有量のヒストグラムからは明らかに組成が粒径に依存していることが示された．とくに細粒な堆積物では SiO_2，K_2O，Ba，Pb，Rb を除くすべての元素がより多く含まれていた．細粒堆積物，粗粒堆積物それぞれの分布のパターンは主に正の歪みを示し，それぞれにはっきりとした違いが見られた．多くの元素(Sr，SiO_2，K_2O，Al_2O_3，CaO，N_2O，Rb)について，砂部分は二峰性または多峰性のパターンを示す．これは局所的な供給源の影響を反映している．とくにモードのうちの 1 つが大山を集水域にもつサンプルと関係している．組成の変化を表したダイアグラムは細粒部分と砂部分で分別が起きていることをはっきりと示している．この結果から，大山からのサンプルは特に Sr 含有量が高く，Y 含有量がかなり低い，起源火山岩のアダカイト質の特徴を反映していることが示された．下流の流路堆積物からは中間的な組成が得られた．そのことは岩相の対照的な 2 つの地域，すなわちフェルシックな花崗岩類と火山岩からなる南部と大山からの火山噴出物からなる北部からの砕屑物が混合，均質化していることを反映している．Cr の値が上流域で高く，このことは超塩基性岩からの供給を強く示唆している．この元素量は下流に向かって安定的に減少するが，それは Cr をあまり含まない砕屑物による希釈を表している．